Synthesis and Recognition Properties of Aromatic Amide Oligomers: Molecular Zippers

ARTICLE *in* JOURNAL OF THE AMERICAN CHEMICAL SOCIETY · AUGUST 2000

Impact Factor: 12.11 · DOI: 10.1021/ja0012671

Synthesis and Recognition Properties of Aromatic Amide Oligomers: Molecular Zippers

Adrian P. Bisson, Fiona J. Carver, Drake S. Eggleston,[†] R. Curtis Haltiwanger,[†] Christopher A. Hunter,* David L. Livingstone,[‡] James F. McCabe, Carmen Rotger,[§] and Alan E. Rowan[||]

Contribution from the Krebs Institute for Biomolecular Science, Department of Chemistry, University of Sheffield, Sheffield S3 7HF, UK, SmithKline Beecham, The Frythe, Welwyn, Hertfordshire AL6 9AR, UK, SmithKline Beecham Pharmaceuticals, 709 Swedeland Road, Philadelphia, Pennsylvania 19406

Received April 11, 2000

Abstract: A series of amide oligomers have been prepared from isophthalic acid and a bisaniline derivative. These compounds assemble into double-stranded zipper complexes in solution via hydrogen-bonding and edge-to-face aromatic interactions. The stability and structures of the complexes have been determined by ^{1}H NMR spectroscopy in chloroform solution. The stability of the complexes increases with increasing chain length, indicating cooperativity between the individual recognition sites in the oligomers. Oligomers which are complementary form more stable complexes than non-complementary systems with overhanging ends. Addition of polar solvents such as methanol destabilizes the complexes, because it competes for hydrogen-bonding interactions which appear to be the main driving force for binding in this system.

Introduction

Self-assembly of linear oligomers into double- and triple- and higher-order multistranded complexes is a common structural motif in biology (Figure 1).[1−3] In addition to its utility for the formation of multicomponent complexes with functional properties, the zipper motif is of fundamental importance for processes such as self-replication and the behavior of biological fibers such as muscle.[4,5] In recent years, chemists have begun to prepare synthetic systems based on this principle. Lehn has used copper coordination by bipyridine oligomers to demonstrate the cooperative assembly of double- and triple-stranded complexes, deMendoza has assembled double-stranded complexes of guanidinium oligomers around sulfate anions, and Anderson has used coordination of DABCO by zinc porphyrins to assemble ladder complexes of porphyrin oligomers.[6−8] We describe here the accidental discovery of a new structural motif which leads to the formation of zipper structures by hydrogen-bonding interactions.[9]

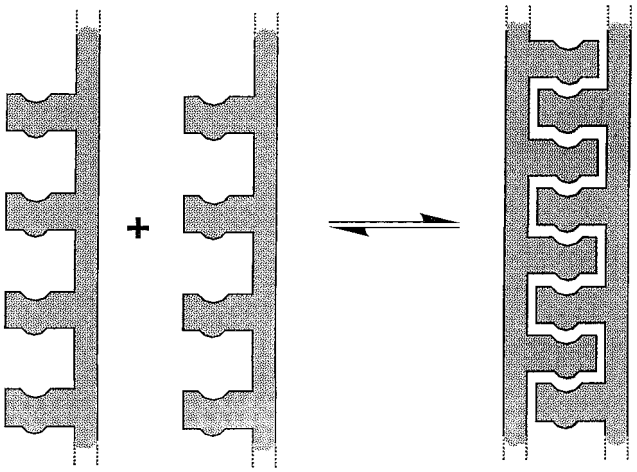

Figure 1. The zipper motif.

[†] SmithKline Beecham, The Frythe, Welwyn, Hertfordshire AL6 9AR, UK.

[‡] SmithKline Beecham Pharmaceuticals, 709 Swedeland Road, Philadelphia, Pennsylvania 19406.

[§] Current address: Department of Chemistry, Universitat de les Illes Balears, 07071 Palma de Mallorca, Spain.

[||] Current address: Department of Organic Chemistry, NSR Centre, University of Nijmegen, The Netherlands.

(1) Horton, R. H.; Moran, L. A.; Ochs, R. S.; Rawn, D. J.; Scrimgeour, G. K. *Principles of Biochemistry*; Prentice Hall International, Inc.: London, 1992.

(2) Pörschke, D. *Biopolymers* **1971**, *10*, 1989−2013; Amirikyan, B. R.; Vologodskii, A. V.; Lyubchenko, Y., L. *Nucleic Acids Res.* **1981**, *9*, 5469−5480.

(3) Wendt, H.; Baici, A.; Bosshard, H. R. *J. Am. Chem. Soc.* **1994**, *116*, 6973−6974; O'Neil, K. T.; Hoess, R. H.; Degrado, W. F. *Science* **1990**, *249*, 774.

(4) Watson, J. D.; Crick, F. H. C. *Nature* **1953**, *4356*, 737−738; von Kiedrowski, G. *Angew. Chem., Int. Ed. Engl.* **1986**, *25*, 932−935; von Kiedrowski, G.; Sievers, D. *Nature* **1994**, *369*, 221−224.

(5) Petruska, J. A.; Hodge, A. J. *Biochemistry* **1964**, *3*, 871−876; Huxley, H. E. *Science* **1969**, *164*, 1356−1364; Davis, J. S.; Buck, J.; Greene, E. P. *FEBS Lett*. **1982**, *140*, 293−297; Huxley, H. E.; Brown, W. *J. Mol. Biol.* **1967**, *30*, 383−434.

(6) Koert, U.; Harding, M. M.; Lehn, J.-M. *Nature* **1990**, *346*, 339; Krämer, R.; Lehn, J.-M.; Cain, A. D.; Fischer, J. *Angew. Chem., Int. Ed. Engl.* **1993**, *32*, 703; Lehn, J.-M.; Rigault, A. *Angew. Chem., Int. Ed. Engl.* **1988**, *27*, 1095; Garret, T. M.; Koert, U.; Lehn, J.-M.; Riguet, A.; Meyer, D.; Fischer, J. *J. Chem. Soc., Chem. Commun.* **1990**, 557; Kramer, R.; Lehn, J. M.; Decian, A.; Fischer, J. *Angew. Chem., Int. Ed. Engl.* **1993**, *32*, 703−706; Zarges, W.; Hall, J.; Lehn, J. M. *Helv. Chim. Acta* **1991**, *74*, 1843−1852; Lehn, J. M. *Pure Appl. Chem.* **1994**, *66*, 1961−1966; Garrett, T. M.; Koert, U.; Lehn, J. M. *J. Phys. Org. Chem.* **1992**, *5*, 529−532; Krämer, R.; Lehn, J. M.; Marquis-Rgault, A. *Proc. Natl. Acad. Sci. U.S.A.* **1993**, *90*, 5394−5398; Pfeil, A.; Lehn, J. M. *J. Chem. Soc., Chem. Commun.* **1992**, 838−840.

(7) SanchezQuesada, J.; Seel, C.; Prados, P.; deMendoza, J.; Dalcol, I.; Giralt, E. *J. Am. Chem. Soc.* **1996**, *118*, 277−278.

(8) Anderson, H. L. *Chem. Commun*. **1999**, 2323−2331; Taylor, P. N.; Anderson, H. L. *J. Am. Chem. Soc.* **1999**, *121*, 11538−11545; Anderson, H. L. *Inorg. Chem.* **1994**, *33*, 972−981; Taylor, P. N.; Huuskonen, J.; Rumbles, G.; Aplin, R. T.; Williams, E.; Anderson, H. L. *Chem. Commun.* **1998**, 909−910.

10.1021/ja0012671 CCC: $19.00
Published on Web 08/30/2000

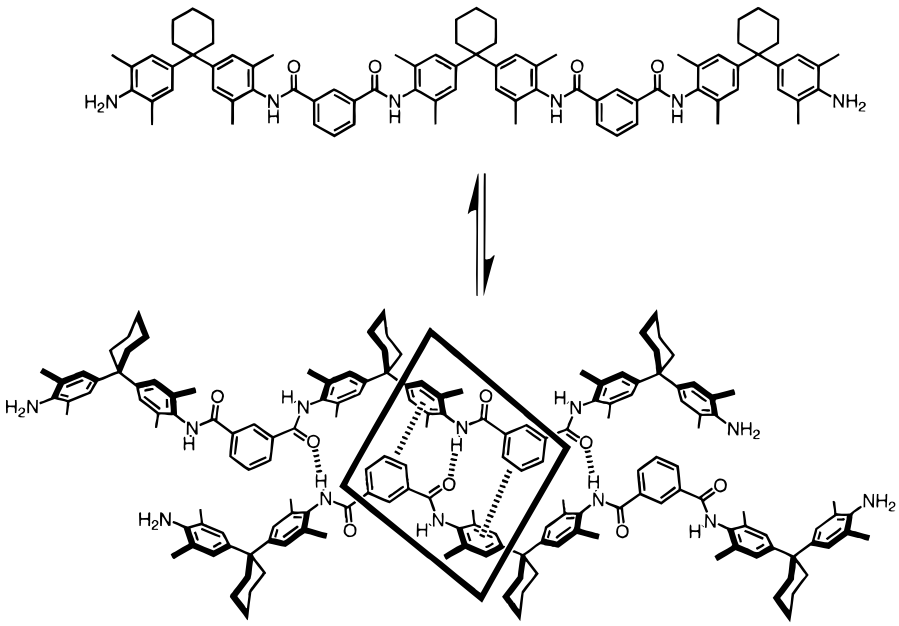

Figure 2. Proposed structure of the oligoamide dimer which accounts for the changes in chemical shift shown in Figure 3. The key structural motif of a hydrogen-bond flanked by two edge-to-face aromatic interactions is highlighted.

Scheme 1

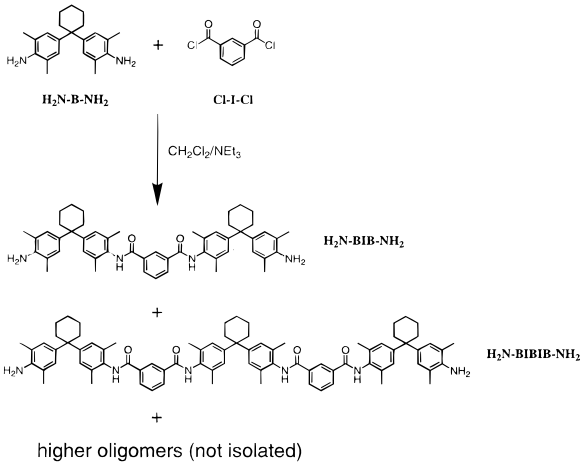

The synthetic route which we have developed to macrocyclic receptors and [2]-catenanes involves the preparation of linear diamides such as **H$_2$N−BIB−NH$_2$** (Scheme 1) which are subsequently cyclized.[10] In Scheme 1, an excess of **H$_2$N−B−NH$_2$** was used to reduce the amounts of higher oligomers formed in this statistical reaction. However, significant amounts of **H$_2$N−BIBIB−NH$_2$** were produced and isolated. The ^{1}H NMR spectrum of this compound in $CDCl_3$ differs significantly from that of the shorter oligomer **H$_2$N−BIB−NH$_2$** (Figure 2): the signals due to the aromatic protons, **t** and **d**, on the isophthaloyl rings show significant upfield shifts in the longer oligomer; the signals due to the amide protons, **n**, are shifted downfield by ∼1 ppm; the signals due to the aniline aromatic protons, **a**, are shifted downfield slightly, and the signal due to the isophthaloyl aromatic singlet, **s**, is unaltered. The shifts were strongly concentration dependent and decreased dramatically on addition of CD_3OD (Figure 2). These observations suggested that the longer oligomer **H$_2$N−BIBIB−NH$_2$** was forming an intermolecular complex which involved H-bonding and aromatic interactions. CPK models were used to construct structures of a dimeric complex consistent with the NMR data (Figure 3). Amide−amide H-bonds lead to downfield shifts of the signals due to the amide protons, **n**. Intermolecular edge-to-face aromatic interactions between the **I** and **B** subunits cause the large upfield shifts on **d** and **t** and the small downfield shift on

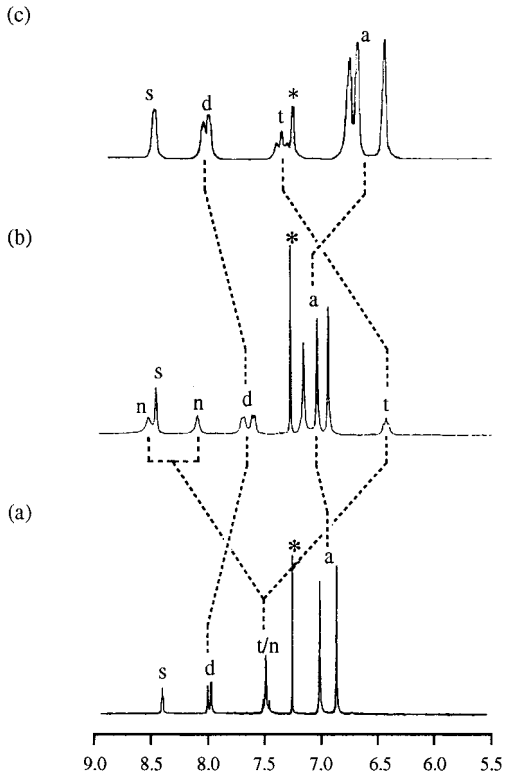

Figure 3. ^{1}H NMR spectra in $CDCl_3$. (a) **H$_2$N−BIB−NH$_2$**, (b) **H$_2$N−BIBIB−NH$_2$**, (c) **H$_2$N−BIBIB−NH$_2$** after the addition of a few drops of CD_3OD.

(9) Bisson, A. P.; Hunter, C. A. *J. Chem. Soc., Chem. Commun.* **1996**, 1723−1724.

(10) Hunter, C. A. *J. Chem. Soc., Chem. Commun.* **1991**, *11*, 749−751; Hunter, C. A.; Purvis, D. H. *Angew. Chem., Int. Ed. Engl.* **1992**, *31*, 792−795; Hunter, C. A. *J. Am. Chem. Soc.* **1992**, *114*, 5303−5311; Carver, F. J.; Hunter, C. A.; Shannon, R. J. *J. Chem. Soc., Chem. Commun.* **1994**, 1277−1280; Adams, H.; Carver, F. J.; Hunter, C. A. *J. Chem. Soc., Chem. Commun.* **1995**, 809−810.

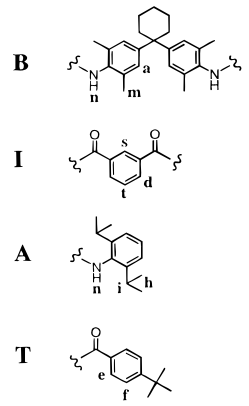

Figure 4. The building blocks used to make the zipper components. The ^{1}H NMR labeling scheme and shorthand subunit nomenclature are also illustrated. Protons which are not labeled in this diagram are unaffected by the formation of zipper complexes.

Scheme 2

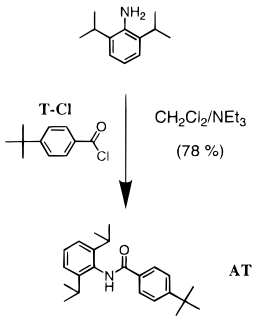

a. **s** is on the outside of the complex and so is unaffected by complexation. However, definitive proof of this zipper structure was elusive.

Assuming that the structure in Figure 3 is accurate, it possible to define the minimal structural motif responsible for recognition in this system: it contains two edge-to-face aromatic interactions and one H-bond (Figure 3). In principle, repeating this monomer unit would afford self-complementary amides of any desired length. We therefore set about synthesising a series of amide oligomers based on this fundamental unit. These systems feature two capping groups, *tert*-butyl benzoyl, **T**, and diisopropyl aniline, **A**, which are used to terminate the **I**−**B** oligomers and differentiate the two components of a complex, facilitating structure determination by two-dimensional ^{1}NMR spectroscopy (Figure 4).

Results and Discussion

Synthesis. The oligomers were prepared according to Schemes 2−8 using sequential acid chloride-aniline amide coupling reactions. Several reactions involve statistical functionalization of one end of a bifunctional molecule, but the reactions can be carried out on a large scale, and the products are easily separated by chromatography. **AIA**, **TBT** and the complex formed between them have been described in detail elsewhere, but the results of the binding experiments are included here for comparison with the other systems.[11]

We have also investigated the use of solid-phase synthesis for the preparation of these compounds (Scheme 9). In this approach, statistical reactions to desymmetrize bifunctional compounds are avoided, and a large excess of reagents can be used to achieve high efficiency in each step. In the first step, isophthaloyl dichloride was attached to the resin by esterification. The following steps involved amide coupling using an alternating sequence of diamine and diacid chloride. Finally, the chain was capped with *tert*-butylbenzoyl chloride, and the resin was cleaved with trifluoroacetic acid. The ^{1}H NMR and mass spectra of the crude products indicated clean formation of the two required zippers shown in Scheme 9, **TBI**−**OH** and **TBIBI**−**OH**. Although this procedure was not used to prepare the compounds discussed below, due to the small scale and the fact that a subsequent coupling reaction is still required to cap the free acid end of the oligomer, this approach offers an attractive alternative for the future preparation of longer zippers of well-defined length without isolating intermediates.

Binding Studies. The assembly of the zipper complexes was investigated using ^{1}H NMR spectroscopy in $CDCl_3/CD_3OD$ (95:5) and $CDCl_3$ where solubility permitted. All of the compounds have concentration dependent ^{1}H NMR spectra. Self-association constants were determined by dilution experiments, and the results are summarized in Table 1. The data could be fit equally well to dimerization or non-cooperative linear polymerization models, but given the evidence for the formation of dimers presented below, the values quoted are for dimeriza-

Scheme 3

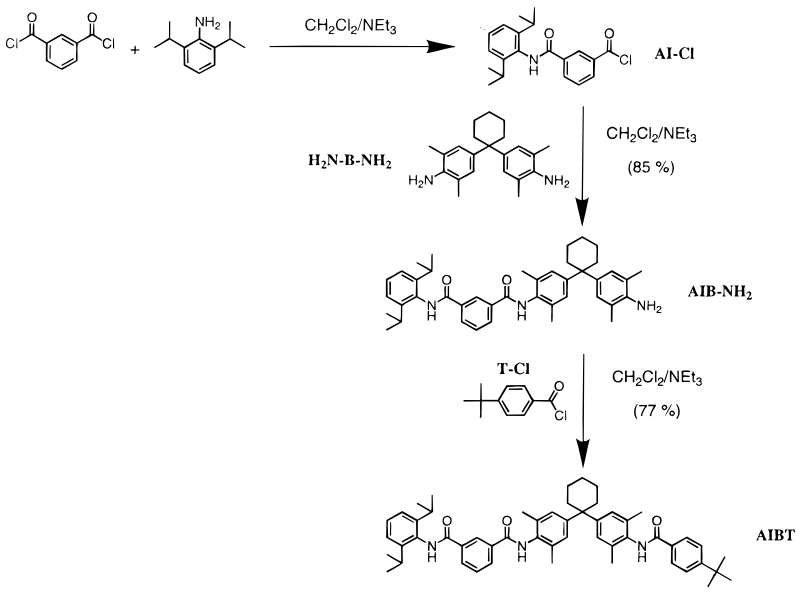

Scheme 4

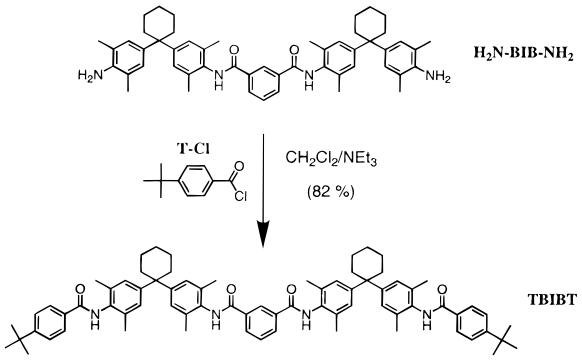

Scheme 5

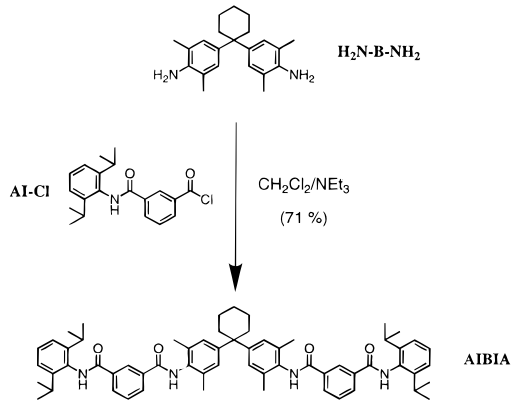

Scheme 6

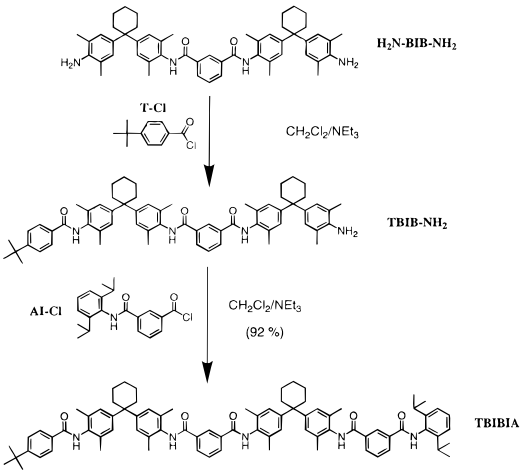

tion. All of the complexes are less stable in the presence of methanol, which suggests that hydrogen-bonding is the main driving force for complexation. There is a significant increase in the magnitude of the self-association constant as the length of the oligomer increases. This reflects the increase in the number of hydrogen-bonding sites as the number of amides increases, but the trend is not uniform along the series. The compounds fall into three distinct groups: **AT**, **AIA**, and **TBT** all have negligible self-association constants; **AIBT**, **AIBIA**, and **TBIBT** have significantly larger self-association constants, and **AIBIBT**, **AIBIBIA**, and **TBIBIBT** self-associate strongly. This observation is consistent with the dimer structures which are shown in Figures 5−7. **AT**, **AIBT**, and **AIBIBT** are self-complementary oligomers and can maximize the number of intermolecular hydrogen-bonds in the dimer. The other dimers all have overhanging ends with amides which are not H-bonded.

Table 1. Self-Association Constants (M^{-1}) from ^{1}H NMR Dilution Experiments (N = Number of Amides in Each Molecule)

compound	N	$CDCl_3/CD_3OD$ (95:5)	$CDCl_3$
AT	1	<1[a]	<1[a]
AIA	2	<1[a]	<1[a]
TBT	2	<1[a]	<1[a]
AIBT	3	20 ± 3	85 ±15
AIBIA	4	26 ± 3	*b*
TBIBT	4	12 ± 2	85 ± 30
AIBIBT	5	1070 ± 190	*b*
AIBIBIA	6	730 ± 200	*b*
TBIBIBT	6	640 ± 170	*b*

[a] Values for these association constants cannot be determined with any relibility because the complexes only reach about 20% saturation at the maximum concentration accessible. [b] Compounds are not sufficiently soluble to perform the experiment.

Consequently, **AT**, **AIA**, and **TBT** form dimers with one hydrogen-bond, **AIBT**, **AIBIA**, and **TBIBT** form dimers with three hydrogen-bonds, and **AIBIBT**, **AIBIBIA**, and **TBIBIBT** form dimers with five hydrogen-bonds, and within each group of compounds, the self-association constants are very similar.

The limiting complexation-induced changes in chemical shift are shown in Table 2. The pattern is very similar to that noted previously for **$H_2N-BIB-NH_2$** and **$H_2N-BIBIB-NH_2$**. The amide protons, **n**, all experience downfield shifts indicative of hydrogen-bonding interactions (the magnitude of this shift is somewhat less in the presence of methanol due to the displacement of hydrogen-bonded solvent). The **d** and **t** protons on the **I** subunits experience upfield shifts, while **s** is unaffected by dimerization. The **a** protons on the **B** subunits experience small downfield shifts. This pattern is characteristic of an edge-to-face interaction between **I** and **B**. Although the data is not complete for each complex, the magnitudes of the changes provide some support for the structures in Figures 5−7. The dimerization-induced changes in chemical shift on the ends of **AIBIA** and **TBIBT** are significantly smaller than the changes observed in the self-complementary systems. In particular, the amide protons move 0.3−0.4 ppm rather than 0.7−0.9 ppm in $CDCl_3/CD_3OD$ (95:5), which suggests that they spend half as much time hydrogen-bonded in the dimer as illustrated in Figure 5.

Further evidence for the structures of the complexes comes from X-ray crystallography.[12,13] The crystal structures of **AT** and **AIA** in Figure 5 show very clearly the basic interaction motif inferred for the complexes in solution: each amide is involved in an intermolecular hydrogen-bond which is flanked by two edge-to-face aromatic interactions. These structures imply that polymerization should take place in solution for **AT** and **AIA**, but the self-association constants for these systems are very small, so at the concentrations studied, the major bound species will be dimer. A 2-dimensional ROESY experiment was performed on **AIBT** at a concentration of 98 mM in $CDCl_3/CD_3OD$ (95:5) (60% dimer), and the clearly identifiable intermolecular NOEs provide good evidence for the zipper structure shown in Figure 5. It is possible that some of the other cross-peaks observed in this experiment are due to intermolecular interactions in the complex; however, it is difficult to distinguish intramolecular from intermolecular NOEs, and the only NOEs shown in Figure 5 are those between protons which are too far apart in the molecule to be caused by intramolecular interactions. The ^{1}H NMR spectrum of **AIBIBT**

(11) Bisson, A. P.; Hunter, C. A.; Morales, J. C.; Young, K. *Chem. Eur. J.* **1998**, *4*, 845−851.
(12) Adams, H.; Carver, F. J.; Hunter, C. A.; Morales, J. C.; Seward, E. M. *Angew. Chem., Int. Ed. Engl.* **1996**, *35*, 1542−1544.

Scheme 7

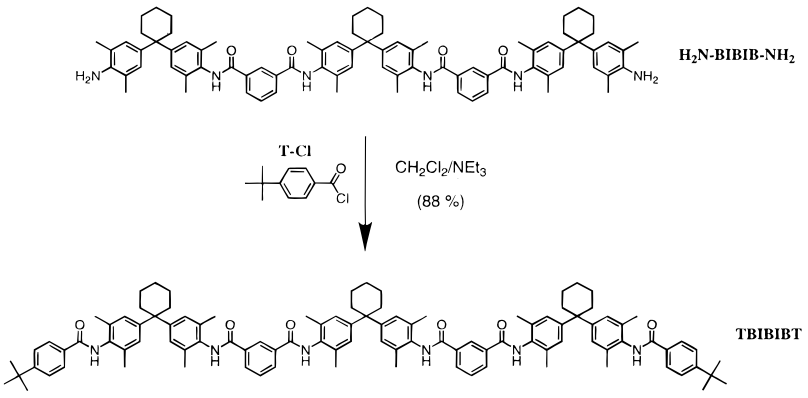

Scheme 8

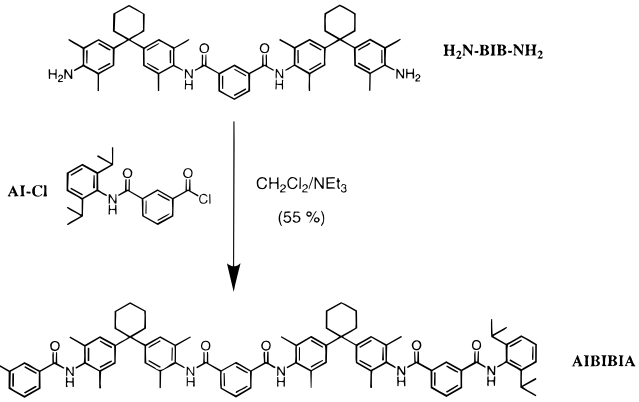

Scheme 9

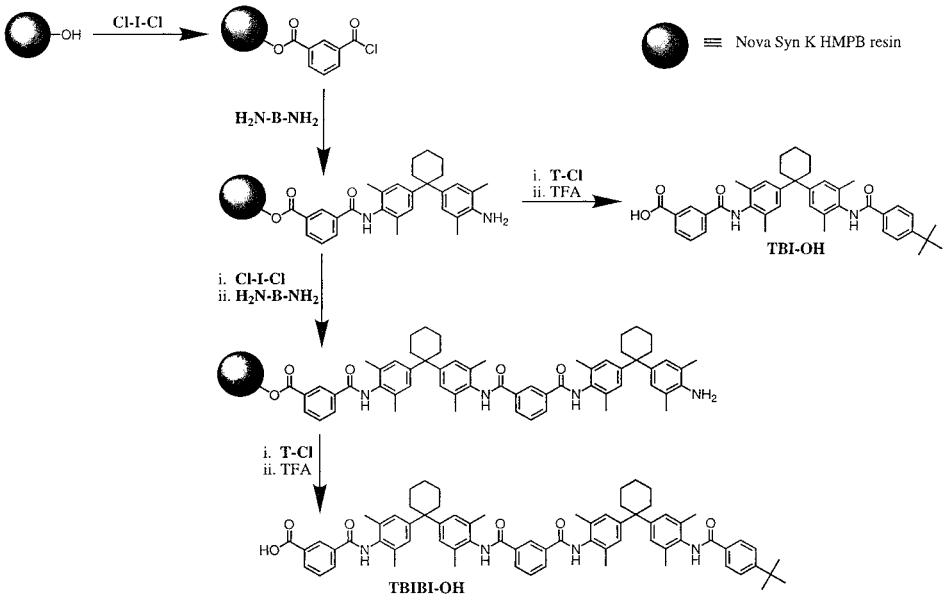

was too broad to permit any useful 2-dimensional experiments on this system. The self-association constant for **AT** is too small for a significant amount of dimer to be present.

The zipper complexes formed by complementary pairs of oligomers were also characterized by ^{1}H NMR spectroscopy using both titration and dilution experiments. The results are summarized in Table 3, and the limiting complexation-induced changes in chemical shift are listed in Table 4. The 1:1 stoichiometry of **AIA·TBT** and **AIBIA·TBIBT** was confirmed by Job plot experiments, but the components of **AIBIBIA·TBIBIBT** were not sufficiently soluble to allow characterization of this complex in the same way. In all three cases, the association constant is more than an order of magnitude larger than the dimerization constants for the individual molecules, confirming the formation of complexes which maximize the number of hydrogen-bonding interactions between complementary partners (Figure 8). Dimerization of the individual components therefore does not complicate analysis of the dilution experiments on the more stable zipper complexes, and the titrations on the less stable zipper complexes were carried out at a concentration where dimerization was insignificant. Reanalysis of the data, taking into account the competing

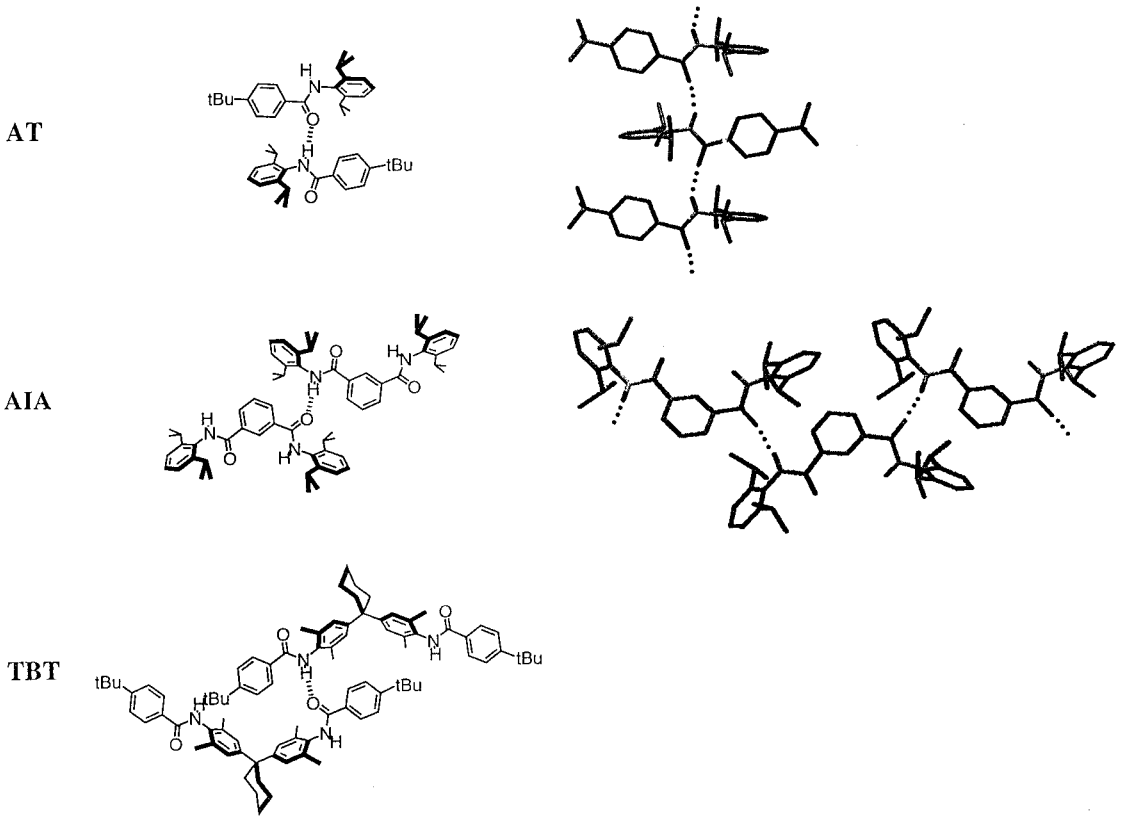

Figure 5. Proposed structures of dimers held together by one hydrogen-bond in solution. Portions of the X-ray crystal structures of **AT** and **AIA** are also shown.

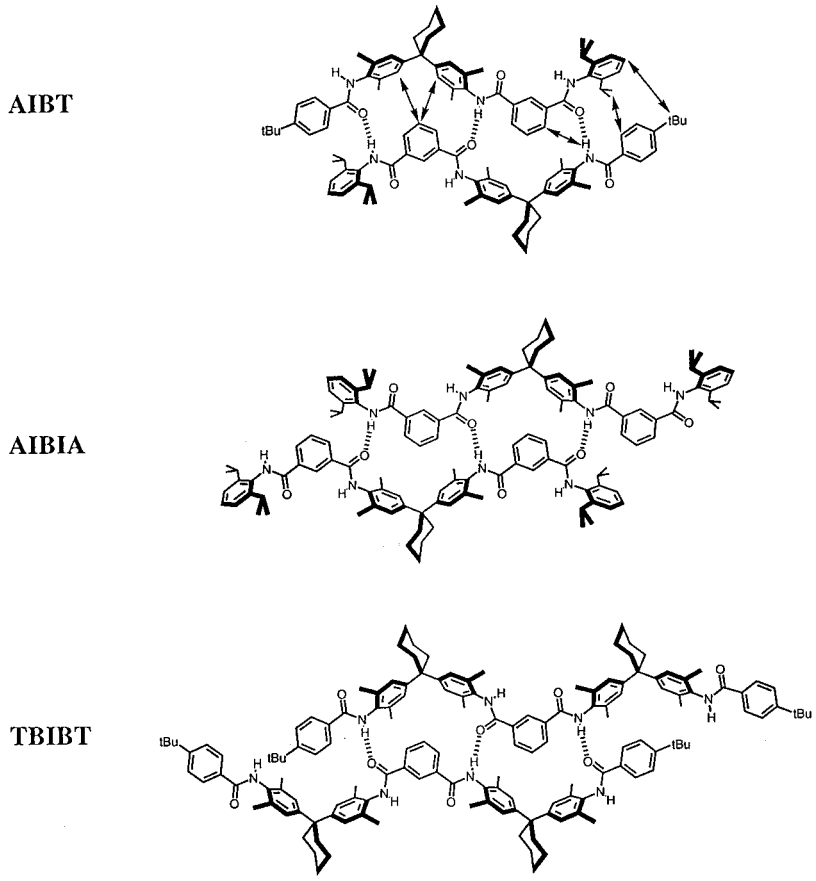

Figure 6. Proposed structures of dimers held together by three hydrogen bonds in solution. Intermolecular NOEs observed in ROESY experiments are shown.

dimerization equilibria, gave very similar results. The ^{1}H NMR spectrum of **AIBIBIA·TBIBIBT** was too broad to allow any useful two-dimensional experiments, but the structures of the other two complexes were confirmed by ROESY experiments

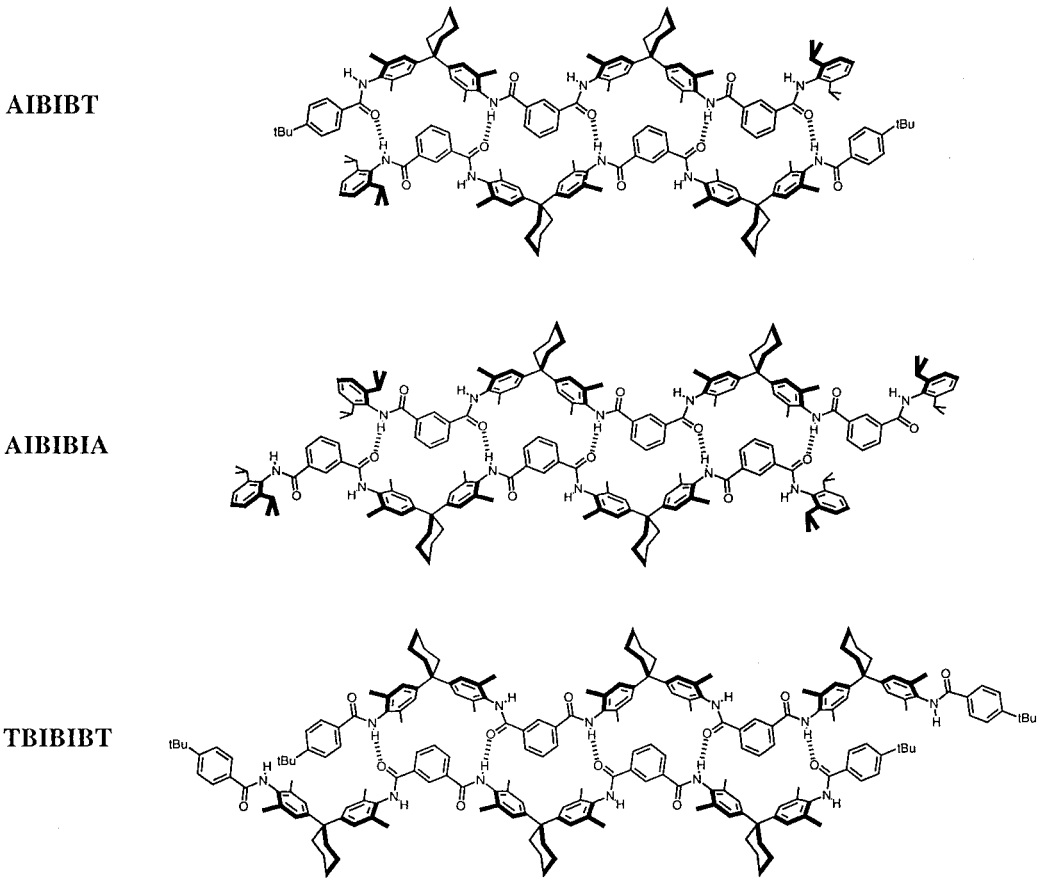

Figure 7. Proposed structures of dimers held together by five hydrogen bonds in solution.

Table 2. Limiting Complexation-Induced Changes in ^{1}H NMR Chemical Shift (ppm) Calculated by Extrapolating Dilution Data for Formation of Dimeric Complexes in $CDCl_3$ and $CDCl_3/CD_3OD$ (95:5) (see Figure 4 for Proton Labeling Scheme)[a]

	amides	A subunit		I subunit			B subunit		T subunit	
compound	**n**	**i**	**h**	**d**	**t**	**s**	**a**	**m**	**e**	**f**
AIBT	+1.8	−0.1	−0.2	−0.4	−1.6	0.0	+0.2	*b*	−0.3	*b*
($CDCl_3$)	+1.5			−0.6			+0.2			
	+1.2									
AIBT	*b*	−0.1	−0.2	−0.6	−1.7	0.0	+0.2	−0.1	−0.3	−0.4
($CDCl_3/CD_3OD$)				−0.6			+0.2	−0.1		
AIBIA	+0.3	*b*	*b*	−0.4	−1.2	0.0	+0.2	0.0		
($CDCl_3/CD_3OD$)	+0.7			−0.5						
TBIBT	+0.4			−0.4	−1.0	0.0	0.0	0.0	−0.1	−0.2
($CDCl_3/CD_3OD$)	+0.7									
AIBIBT	+0.9	0.0	0.1	−0.3	−1.5	0.0	+0.2	*b*	−0.2	*b*
($CDCl_3/CD_3OD$)					−1.5					
AIBIBIA	+0.7	*b*	*b*	*b*	−1.5	0.0	*b*	*b*		
($CDCl_3/CD_3OD$)					−1.6					
TBIBIBT	*b*			−0.4	−1.1	0.0	+0.1	*b*	−0.1	−0.1
($CDCl_3/CD_3OD$)										

[a] Errors are of the order of ±20%. Where more than one proton was observed in each category, these are listed in order from the end of the zipper (starting with the **A** subunit) toward the other end or toward the center in symmetrical systems. In many cases, the different protons within a class were not resolved in the spectrum, and the number quoted represents an composite value for the multiplet. [b] These signals were not sufficiently well-resolved during the titration/dilution experiment to allow determination of reliable chemical shift changes.

(Figure 8). The limiting complexation-induced changes in chemical shift show exactly the same pattern as discussed for the other complexes and confirm that these systems adopt the same zipper structure (Table 4). We have used the complexation-induced changes in chemical shift for **AIA·TBT** to determine the full three-dimensional structure of the complex in solution, and this agrees with qualitative interpretation of the data shown in Figure 8.[14]

These experiments all show that the amide oligomers form dimeric zipper complexes in solution. The data for complementary binding partners are collected in Table 5. The average complexation-induced changes in chemical shift for the different classes of proton are essentially identical indicating that

Table 3. Association Constants (M^{-1}) from ^{1}H NMR Dilution and Titration Experiments

complex	$CDCl_3/CD_3OD$ (95:5)	$CDCl_3$
AIA·TBT	18 ± 3^a	45 ± 1^a
AIBIA·TBIBT	240 ± 11^a	14000 ± 6000^b
AIBIBIA·TBIBIBT	55000 ± 35000^b	*c*

[a] Measured by a titration experiment. [b] Measured by a dilution experiment. [c] Neither the compounds nor the complex are sufficiently soluble to be studied in this solvent.

Table 4. Limiting Complexation-Induced Changes in ^{1}H NMR Chemical Shift (ppm) Calculated by Extrapolating Dilution or Titration Data for Formation of a 1:1 Complex (see Figure 4 for Proton Labeling Scheme)[a]

	amides	A subunit		I subunit			B subunit		T subunit	
complex	**n**	**i**	**h**	**d**	**t**	**s**	**a**	**m**	**e**	**f**
AIA	+1.4	−0.1	−0.2	−0.4	−1.6	0.0				
TBT	+1.1						+0.2	0.0	−0.3	−0.5
($CDCl_3$)										
AIA	+0.6	−0.1	−0.1	−0.4	−1.6	0.0				
TBT	*b*						+0.2	0.0	−0.3	−0.5
($CDCl_3$/CD_3OD)										
AIBIA	*b*	−0.1	−0.2	−0.4	−1.8	0.0	+0.2	0.0		
TBIBT	*b*			−0.4	−1.8	0.0	+0.2	0.0	−0.2	*b*
($CDCl_3$)							+0.3			
AIBIA	+0.5	0.0	−0.1	−0.4	−1.4	0.0	+0.1	0.0		
	+0.5			−0.5						
TBIBT	+0.5			−0.5	−1.3	0.0	+0.1	0.0	−0.2	−0.3
($CDCl_3$/CD_3OD)	+0.4						+0.1	−0.1		
AIBIBIA·TBIBIBT	*b*	*b*	−0.1	*b*	*b*	*b*	+0.2	*b*	*b*	*b*
($CDCl_3$/CD_3OD)										

[a] Errors are of the order of ±20%. Where more than one proton was observed in each category, these are listed in order from the end of the zipper toward the center. In some cases, the different protons within a class were not resolved in the spectrum, and the number quoted represents an composite value for the multiplet. [b] These signals were not sufficiently well-resolved during the titration/dilution experiment to allow determination of reliable chemical shifts.

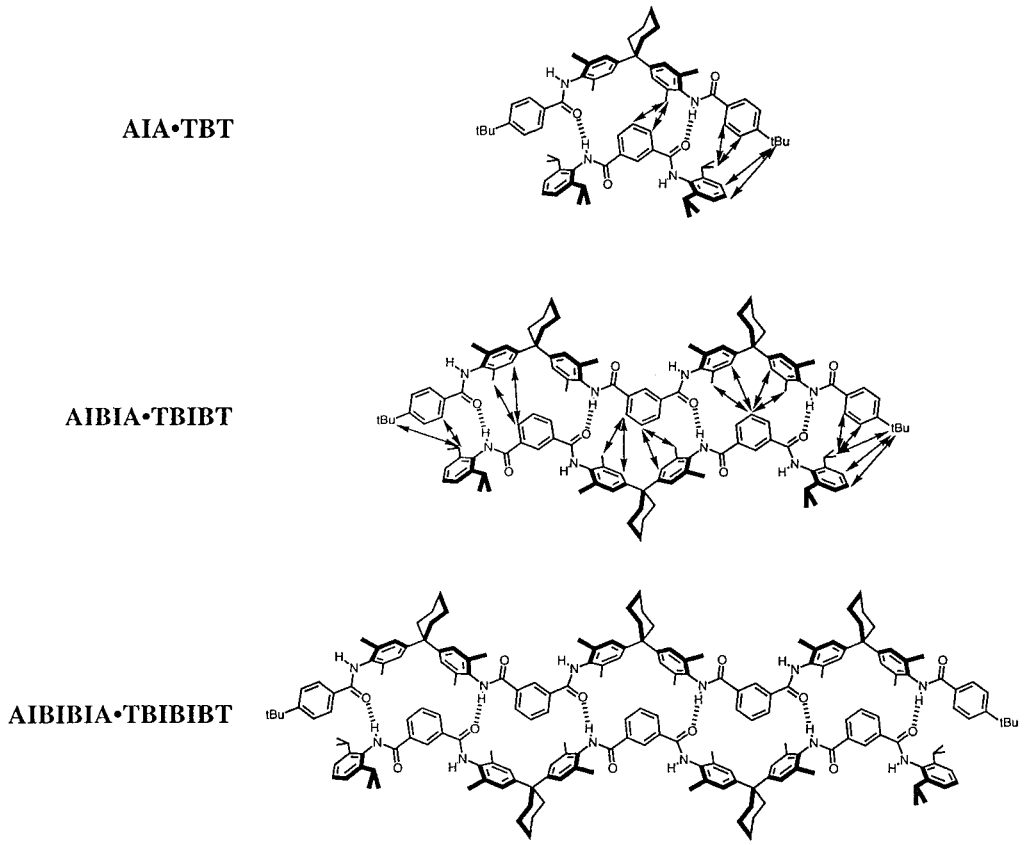

Figure 8. Proposed structures of the zipper complexes formed between two complementary but different oligomers. Intermolecular NOEs observed in ROESY experiments are shown.

the complexes all have similar structures. The stability of the complexes (ΔG_{obs}) increases with the length of the oligomer and decreases on addition of competitive hydrogen-bonding solvents such as methanol. Although, complementary binding partners form the most stable complexes, non-complementary oligomers will bind. For example, we have carried out a titration of **AIA** into **TBIBT** in $CDCl_3$ at a concentration where **TBIBT** is not significantly dimerized. A Job plot indicates that the stoichiometry of the complex is 2:1 (the maximum occurs for a mole fraction of approximately 0.6 **AIA**), and the microscopic association constants for the first and second binding interactions are 40 ± 4 M^{-1} and 50 ± 6 M^{-1} respectively (Figure 9). These binding constants are essentially identical to the value for the **AIA·TBT** complex in chloroform (Table 3), and the complexation-induced changes in chemical shift are also very similar to those observed for the **AIA·TBT** complex (Table 4, Figure 9). This indicates that **AIA** binds to **TBIBT** in exactly the same way as it binds to **TBT**, and that the binding of the first molecule of **AIA** has no effect on the second binding site. This augurs well for the use of these molecules in template-directed synthesis.

Figure 10 shows how the stability of the zipper complexes

Table 5. Summary of Complexation Data for Complementary Zipper Complexes. Average Complexation-Induced Changes in Chemical Shift (ppm), Observed Free Energy of Binding, ΔG_{obs}, and Statistically Corrected Free Energy of Binding, ΔG_c, (kJ mol^{-1}) in $CDCl_3$ and $CDCl_3$/CD_3OD (95:5)

	proton[†]						$CDCl_3$		$CDCl_3/CD_3OD$	
complex	e	f	a	h	d	t	ΔG_{obs}	ΔG_c	ΔG_{obs}	ΔG_c
AIA·TBT	−0.3	−0.5	+0.2	−0.1	−0.4	−1.6	9.5 ± 0.1	7.8 ± 0.1	7.2 ± 0.4	5.5 ± 0.4
(AIBT)$_2$	−0.3	−0.4	+0.2	−0.2	−0.6	−1.7	11.1 ± 0.4	11.1 ± 0.4	7.5 ± 0.4	7.5 ± 0.4
AIBIA·TBIBT	−0.2	−0.3	+0.2	−0.1	−0.4	−1.6	23.7 ± 1.0	22.1 ± 1.0	13.7 ± 0.1	11.9 ± 0.1
(AIBIBT)$_2$	−0.2	*b*	+0.2	−0.1	−0.3	−1.5	−	−	17.4 ± 0.4	17.4 ± 0.4
AIBIBIA·TBIBIBT	*b*	*b*	+0.2	−0.1	*b*	*b*	−	−	27.2 ± 1.6	25.5 ± 1.6

[a] See Figure 4 for ^{1}H NMR labeling scheme. The average value for each class of proton is quoted. [b] These signals were not sufficiently well-resolved during the titration/dilution experiment to allow determination of reliable chemical shifts.

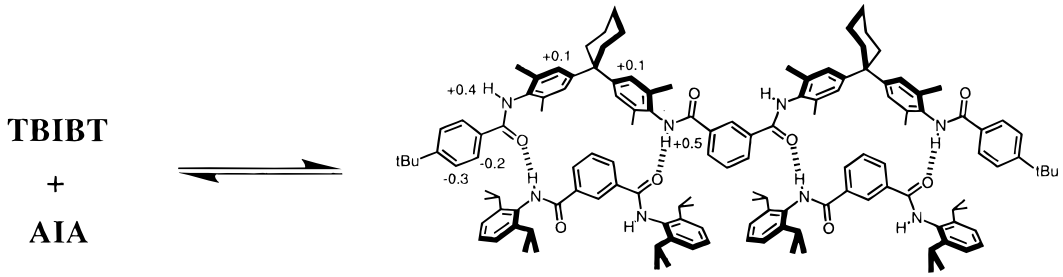

Figure 9. The 2:1 complex formed between **AIA** and **TBIBT**. The limiting complexation-induced changes in chemical shift are shown.

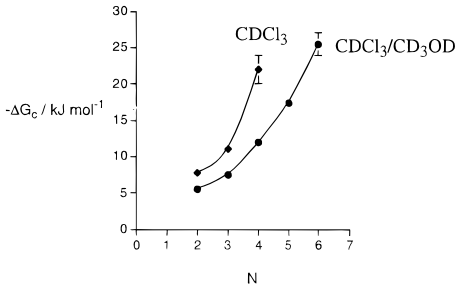

Figure 10. The statistically corrected free energy of binding in $CDCl_3$ and $CDCl_3/CD_3OD$ (95:5) ($-\Delta G_c$) plotted against the length of the oligomer (*N*). *N* is the number of repeats of the recognition motif (two edge-to-face $\pi-\pi$ interactions and one hydrogen bond). Error bars for most of the points lie within the symbol. The curve illustrates the trend and is not a fit to any function.

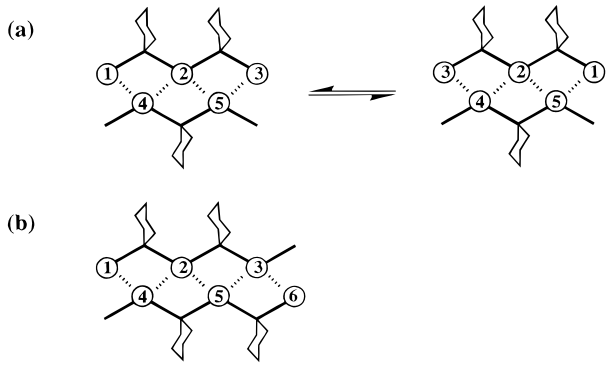

Figure 11. Schematic representations of (a) the heterodimeric zipper **AIBIBT** and (b) the homodimeric zipper **AIBIA·TBIBT**. The **I** and **T** groups in each complex are numbered to allow differentiation of degenerate conformations. The heterodimeric complexes can adopt two different types of conformation, whereas the homodimeric zippers can only adopt one.

(ΔG_c) increases as the number of binding interactions (*N*) increases. The data in this graph have been corrected for statistical effects: the components of the homodimeric zipper complexes are directional, and these complexes can therefore only be assembled in a head-to-tail arrangement. The heterodimeric complexes, on the other hand, are composed of symmetrical molecules and can therefore be assembled in two different degenerate conformations (Figure 11). Thus, to make a true comparison of the stability constants, the statistical term has been factored out by dividing the association constants for the heterocomplementary systems by 2 (to give ΔG_c in Table 5).[9] A smooth trend is only observed when this correction is applied to the data, that is, ΔG_{obs} does not follow the same pattern. The graph in Figure 10 appears to have a slight curvature, but there is insufficient data to draw any firm conclusions. The upward curvature could be caused by fraying at the ends of the zipper or by positive enthalpic cooperativity, so that the addition of further binding interactions causes a greater increase in stability than the addition of previous binding interactions. Williams has shown that positive enthalpic cooperativity of this sort is reflected in the complexation-induced changes in chemical shift, but in our system, this effect is not

(13) **AIA** crystallized as colorless prisms from a mixture of acetonitrile and ethanol, and there is one molecule of ethanol solvate per molecule of **AIA** in the crystal. Lattice parameters were determined from the setting angles of 25 reflections well distributed in reciprocal space measured on an Enraf Nonius CAD-4 diffractometer. Intensity data were collected on the diffractometer using graphite monochromated molybdenum radiation and an $\omega - 2\theta$ variable speed scan technique. Three orientation controls were monitored to assess any crystal movement during the experiment. The intensities of three standard reflections measured at the beginning, end and every hour of exposure time showed a variation of 8% over the course of the experiment. Data were corrected for this variation and for Lorentz and polarization effects. Equivalent reflections were averaged. Crystal data and refinement details are presented in Table 1 of the Supporting Information. The structure was solved by direct methods using the SHELXS program and refined using the SHELXL-93 program. Atomic positions were eventually refined with anisotropic displacement parameters. Parameters for hydrogen attached to nitrogen were refined. Other hydrogen atoms were included in idealised positions which rode on the atom to which they are attached. Isotropic displacement factors were assigned as a constant (1.2) times Ueq of the attached atom. The full-matrix least-squares refinement (on E^2) converged ($\Delta/\sigma_{max} = 0.00$) to values of the conventional crystallographic residuals R = 0.046 for observed data and R = 0.058 (wR2 = 0.140) for all data. The function minimized was $\Sigma w(F_o^2 - F_c^2)^2$. Weights, *w*, were eventually assigned to the data as $w = 1/[\sigma^2(F_o^2) + (0.0670P)^2 + 1.8373P]$ where $P = [MAX(F_o^2, 0) + 2F_c^2]/3$. A final difference Fourier map was featureless with residual density between +0.36 and −0.21 eÅ^{-3}. Values of the neutral atom scattering factors were taken from the International Tables for X-ray Crystallography.

(14) Hunter, C. A.; Packer, M. J. *Chem. Eur. J.* **1999**, *5*, 1891−1897.

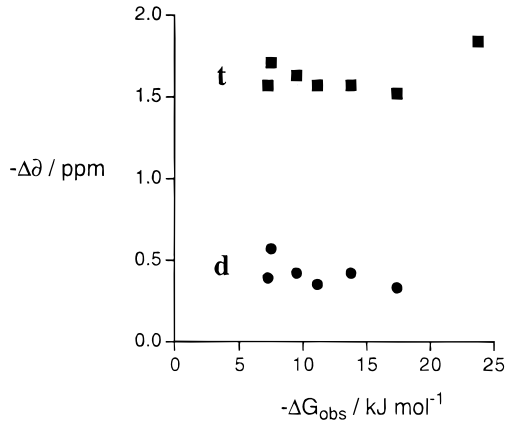

Figure 12. Average limiting complexation-induced changes in chemical shift of protons **d** and **t** ($\Delta\partial$) plotted as a function of the stability of the zipper complexes ($-\Delta G_{obs}$).

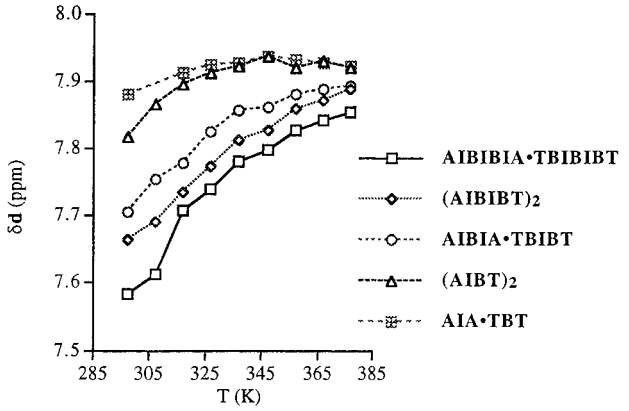

Figure 13. Melting curves for the zipper complexes in $CDCl_3/CD_3OD$ (95:5). The curves simply illustrate the trends and do not represent fits to a specific function.

observed. Figure 12 shows how the average limiting complexation-induced changes in chemical shift for signals **t** and **d** vary as a function of the overall free energy of binding: both values are essentially constant.

Cooperative assembly of zipper motifs can be characterized by a cooperative melting transition when the system is heated.[2,6] Melting of the zipper complexes was investigated by variable temperature ^{1}H NMR spectroscopy in $CDCl_3/CD_3OD$ (95:5). The average chemical shift the signals due to the **d** protons was monitored over the range 297−377 K, and the results are plotted in Figure 13. The complexes clearly dissociate on heating, and the more stable complexes are more difficult to dissociate, but the fully associated low-temperature limit is difficult to reach, and so it is not possible to draw any conclusions about the shape of the melting curves or the extent of cooperativity.

Conclusions

The amide oligomers formed from isophthalic acid and bisaniline, **H$_2$N−B−NH$_2$**, assemble into stable double-stranded complexes held together by hydrogen-bonding interactions. As the length of the oligomer increases, the stability of the corresponding complex increases, indicating significant cooperativity in the intermolecular interactions along the chain. Selectivity in recognition relies entirely on length in this system, since the stability is determined solely by the number of hydrogen-bonding interactions that can be made. Future work will focus on methods for engineering sequence-selectivity into the zipper assembly process.

Experimental Section

The preparation of **H$_2$N−B−NH$_2$**, **AIA**, and **TBT** have been described previously.[10,11] All other reagents were purchased from the Aldrich Chemical Co. and used without further purification. The ^{1}H NMR signals are assigned using the subunit identifiers, **A**, **B**, **I**, and **T**, to indicate the location the corresponding proton in a particular part of the molecule.

Synthesis of AT. Et_3N (2.25 mmol; 0.31 mL) and 2,6-diisopropyl aniline (1.5 mmol; 0.28 mL) were dissolved in dry CH_2Cl_2 (15 mL). *tert*-Butyl benzoyl chloride (2.25 mmol; 0.42 mL) was then added dropwise over 10 min. The reaction was allowed to stir for 10 hours and then washed with 1 M HCl (2 × 25 mL) and 1 M NaOH (2 × 25 mL). The organic phase was then dried over Na_2SO_4 (anhydrous). The Na_2SO_4 was removed by filtration and the organic phase reduced to dryness on a rotary evaporator. The yellow solid produced was recrystallized from CH_2Cl_2/pet ether (40−60) to yield the desired product as a white solid (589 mg; 78%); mp > 270 °C. δ_H in $CDCl_3$ (ppm): 7.88(d, 2H, **T** Ar−CH); 7.65(s, 1H, NH); 7.52(d, 2H, **T** Ar−CH); 7.35(t, 1H, **A** Ar−CH); 7.20(d, 2H, **A** Ar−CH); 3.15(sept, 2H, **A** C$\underline{H}$Me$_2$); 1.35(s, 9H, **T** C$\underline{Me}_3$); 1.20(d, 12H, **A** CH$\underline{Me}_2$). δ_C in $CDCl_3$ (ppm): 166.5; 154.9; 146.7; 133.3; 132.0; 128.1; 127.8; 125.7; 123.4; 35.1; 31.4; 28.7; 24.0; 23.7. FAB[+ve] m/z = 338, $C_{23}H_{31}NO$ requires 337. CHN: Calculated C = 81.90, H = 9.20, N = 4.15. Found C = 81.83, H = 9.30, N = 4.08.

Synthesis of AI−COCl. A mixture of 2,6-diisopropylaniline (5.0 g, 0.03 mol) and triethylamine (5.75 mL, 0.04 mol) in CH_2Cl_2 (50 mL) was added in a dropwise fashion to a stirred solution of isophthaloyl dichloride (84 g, 0.4 mol) in CH_2Cl_2 (200 mL) over a 3 h period at room temperature. Following the addition, the mixture was stirred at room temperature for a further 20 h, before concentration in vacuo and purification by flash column chromatography (CH_2Cl_2:cyclohexane). Recrystallization from CH_2Cl_2/pet ether(40−60) gave **AI−COCl** as cream needles (8.2 g, 86%); mp 178−179 °C. δ_H in $CDCl_3$ (ppm): 8.65(s, 1H, **I** Ar−CH); 8.35(d, 1H, **I** Ar−CH); 8.22(d, 1H, **I** Ar−CH); 7.65(t, 1H, **I** Ar−CH); 7.60(s, 1H, NH); 7.40(t, 1H, **A** Ar−CH); 7.25-(d, 2H, **A** Ar−CH); 3.10(sept, 2H, **A** C$\underline{H}$Me$_2$); 1.2(d, 12H, **A** CH$\underline{Me}_2$). δ_C in $CDCl_3$ (ppm): 170.0; 165.4; 146.3; 135.4; 134.2; 133.7; 130.8; 129.7; 129.6; 128.7; 128.4; 123.6; 29.0; 23.6. FAB[+ve] m/z = 344, $C_{20}H_{22}NO_2Cl$ requires 343. IR in $C_2H_2Cl_4$ solution (cm^{-1}): 3422; 2992; 2981; 1753; 1678; 1600; 1495; 1471;1423; 1387; 1364. CHN: Calculated C = 69.97, H = 6.41, N = 4.08. Found C = 69.69, H = 6.37, N = 3.86.

Synthesis of TB−NH$_2$. Et_3N (1.0 mL, 0.0137 mol) and **H$_2$N−B−NH$_2$** (8.43 g, 0.0262 mol) were dissolved in dry CH_2Cl_2 (75 mL). To this vigorously stirring solution was added dropwise over 5 h a solution of *tert*-butyl benzoyl chloride (0.7 mL, 3.74 mmol) in dry CH_2Cl_2 (225 mL). The reaction was allowed to stir overnight before being washed with 1 M HCl (2 × 300 mL) to remove the excess **H$_2$N−B−NH$_2$**. The organic phase was dried over Na_2SO_4 (anhydrous) and then filtered. Flash column chromatography on silica, eluting with 60% pet ether (40−60)/ethyl acetate, yielded the product as the first major band. Recrystallization from CH_2Cl_2/pet ether(40−60) gave a white solid (0.873 g, 49%); mp 251−252 °C. δ_H in 5% CD_3OD in $CDCl_3$ (v/v) (ppm): 7.75(d, 2H, **T** Ar−CH); 7.44(d, 2H, **T** Ar−CH); 6.92(s, 2H, **B** Ar−CH); 6.80(s, 2H, **B** Ar−CH); 2.20(m, 16H, **B** Me, **B** c-hexyl); 1.50−1.40(m, 6H, **B** c-hexyl); 1.55(s, 18H, **T** C$\underline{Me}_3$). δ_C in d_6-DMSO (ppm): 165.3; 154.7; 148.1; 140.8; 136.7; 135.3; 132.8; 132.2; 127.8; 126.7; 126.4; 125.6; 121.6; 44.6; 37.0; 35.1; 31.4; 26.4; 23.1; 18.9; 18.7. FAB[+ve] m/z = 482, $C_{33}H_{42}N_2O$ requires 482. IR in $C_2H_2Cl_4$ solution (cm^{-1}): 3459; 2937; 2860; 1646; 1566; 1524; 1493; 1375.

Synthesis of AIB−NH$_2$. H$_2$N−B−NH$_2$ (5.93 mmol; 1.9 g) and Et_3N (0.593 mmol; 82 μl) were dissolved in dry CH_2Cl_2 (25 mL), and to this solution was added dropwise over 3 h the **AI−COCl** (203 mg, 0.593 mmol) in CH_2Cl_2 (75 mL). The reaction was allowed to stir for 5 h. Flash column chromatography on silica, eluting with 1% EtOH/CH_2Cl_2, yielded the desired product and the excess **H$_2$N−B−NH$_2$** as the first major band. These mixed fractions were then washed with 1 M HCl (2 × 500 mL) to remove the excess **H$_2$N−B−NH$_2$** and then dried over Na_2SO_4 (anhydrous). The Na_2SO_4 was removed by filtration and the organic solution reduced to dryness on the rotary evaporator,

to yield the desired product as a white solid (0.32 g; 85%); mp >270 °C. δ_H in 5% CD_3OD in $CDCl_3$ (v/v) (ppm): 8.60(s, 1H, NH); 8.49(s, 1H, **I** Ar−CH);8.40(s, 1H, NH); 8.06(m, 2H, **I** Ar−CH); 7.51(t, 1H, **I** Ar−CH); 7.36(t, 1H, **A** Ar−CH);7.23(d, 2H, **A** Ar−CH); 7.03(s, 2H, **B** Ar−CH); 6.85(s, 2H, **B** Ar−CH); 3.15(sept, 2H, **A** C$\underline{H}$Me$_2$); 2.23-(m, 10H, **B** Me, **B** c-hexyl); 2.15(s, 6H, **B** Me); 1.65−1.55(m, 6H, **B** c-hexyl); 1.20(d, 12H, **A** CH$\underline{Me}_2$). δ_C in $CDCl_3$ (ppm): 166.0; 165.0; 148.8; 146.4; 140.1; 135.2; 135.0; 134.7; 130.8; 130.6; 130.3; 129.4; 128.7; 127.1; 126.0; 123.6; 121.5; 44.9; 37.2; 28.9; 26.5; 23.7; 23.0; 18.9; 18.1. FAB[+ve] m/z = 630, $C_{42}H_{51}N_3O_2$ requires 629. IR in KBr disk (cm^{-1}): 3429; 2961; 2934; 2863; 1648; 1510; 1471; 1383; 1362.

Synthesis of AIBT. The **AIB−NH$_2$** (1.89×10^{-4} mol; 119 mg) and Et_3N (2.84×10^{-4} mol; 40 μl) were dissolved in dry CH_2Cl_2 (10 mL). *tert*-Butyl benzoyl chloride (2.84×10^{-4} mol; 53 μl) was then added and the reaction allowed to stir for 5 h. The reaction was then washed with 1 M HCl (2 × 20 mL) and 1 M NaOH (2 × 20 mL) before the organic phase was dried over Na_2SO_4 (anhydrous). The Na_2SO_4 was removed by filtration and the organic solution reduced to dryness on the rotary evaporator, to yield a yellow solid. The products were separated by preparative TLC mixture eluting with 2% EtOH/CH_2Cl_2 to yield the desired product as the lowest band. The product was recrystallized from CH_2Cl_2/pet ether(40−60) to give a white solid (115 mg; 77%); mp 214−215 °C. δ_H in d_6-DMSO (ppm): 9.90(s, 1H, NH); 9.85(s, 1H, NH); 9.55(s, 1H, NH); 8.55(s, 1H, **I** Ar−CH); 8.20-(m, 2H, **I** Ar−CH); 7.92(d, 2H, **T** Ar−CH); 7.70(t, 1H, **I** Ar−CH); 7.53(d, 2H, **T** Ar−CH); 7.37(t, 1H, **A** Ar−CH); 7.23(d, 2H, **A** Ar−CH); 7.10(s, 4H, **B** Ar−CH); 3.15(sept, 2H, **A** C$\underline{H}$Me$_2$); 2.30(m, 4H, **B** c-hexyl); 2.22(s, 6H, **B** Me); 2.15(s, 6H, **B** Me); 1.65−1.55(m, 6H, **B** c-hexyl); 1.35(s, 9H, **T** C$\underline{Me}_3$); 1.20(2d,12H, **A** CH$\underline{Me}_2$). δ_C in d_6-DMSO (ppm): 166.2; 165.2; 165.1; 154.7; 147.2; 146.9; 146.6; 135.6; 135.5; 135.4; 135.3; 133.2; 133.1; 132.9; 132.1; 130.6; 129.2; 128.2; 127.8; 127.6; 126.6; 125.7; 123.4; 45.2; 36.7; 31.4; 28.7; 26.3; 24.0; 23.8; 23.2; 19.0. FAB[+ve] m/z = 791, $C_{53}H_{63}N_3O_3$ requires 789. IR in $C_2H_2Cl_4$ solution (cm^{-1}): 3422; 2992; 2980; 2969; 2937; 2867; 1668; 1609; 1490; 1470; 1383.

Synthesis of AIBIA. AI−COCl (3.30 mmol; 1.13 g) was dissolved in dry CH_2Cl_2 (15 mL), and to this solution was added over 20 min a solution of **H$_2$N−B−NH$_2$** (1.32 mmol; 425 mg) and Et_3N (3.95 mmol; 0.55 mL) in dry CH_2Cl_2 (30 mL). The reaction was allowed to stir for 2 h and then washed with 1 M HCl (2 × 200 mL), 1 M NaOH (2 × 200 mL), and water (2 × 200 mL). The organic phase was then dried over Na_2SO_4 (anhydrous). The Na_2SO_4 was removed by filtration and the organic solution reduced to dryness on the rotary evaporator. Flash column chromatography on silica, eluting with 1% EtOH/CH_2Cl_2, gave the desired product as the third band. The product was recrystallized from CH_2Cl_2/MeOH/pet ether (40−60) to give a white solid (876 mg; 71%); mp >270 °C. δ_H in 5% CD_3OD in $CDCl_3$ (v/v) (ppm): 8.52(s, 2H, **I** Ar−CH); 8.15(m, 4H, **I** Ar−CH); 7.57(t, 2H, **I** Ar−CH); 7.35(t, 2H, **A** Ar−CH); 7.22(d, 2H, **A** Ar−CH); 7.13(s, 4H, **B** Ar−CH); 3.15-(sept, 2H, **A** C$\underline{H}$Me$_2$); 2.25(m, 16H, **B** Me, **B** c-hexyl); 1.65−1.45(m, 6H, **B** c-hexyl); 1.22(d, 12H, **A** CH$\underline{Me}_2$). δ_C in d_6-DMSO (ppm): 166.2; 165.2; 147.2; 146.6; 135.5; 135.4; 135.2; 133.1; 133.0; 130.6; 129.2; 128.2; 127.5; 126.6; 123.5; 45.2; 36.7; 28.7; 23.8; 23.5; 23.2; 19.0. FAB[+ve] m/z = 937, $C_{62}H_{72}O_4N_4$ requires 936. IR in $C_2H_2Cl_4$ solution (cm^{-1}): 3414; 3295; 2994; 2933; 2866; 1646; 1584; 1517; 1496; 1469.

Synthesis of H$_2$N−BIB−NH$_2$, H$_2$N−BIBIB−NH$_2$. H$_2$N−B−NH$_2$ (33.67 mmol; 10.857 g) and Et_3N (10.36 mmol; 1.44 mL) were dissolved in dry CH_2Cl_2 (50 mL). To this solution was added dropwise over 2 h a solution of isophthaloyl dichloride (5.179 mmol; 1.05 g) in dry CH_2Cl_2 (100 mL). The reaction was then left to stir for 8 h. Flash column chromatography on silica, eluting with 100% $CHCl_3$ and finally 2.0% EtOH/$CHCl_3$, yielded **H$_2$N−BIB−NH$_2$** as the second band (white solid 2.94 g; 73%) and **H$_2$N−BIBIB−NH$_2$** as the third band (white solid 671 mg; 11%). The first band was unreacted **H$_2$N−B−NH$_2$**.

H$_2$N−BIB−NH$_2$: mp 179−180 °C. δ_H in $CDCl_3$ (ppm): 8.45(s, 1H, **I** Ar−CH); 8.00(d, 2H, **I** Ar−CH); 7.50(m, 3H, NH, **I** Ar−CH); 7.20(s, 2H, **B** Ar−CH); 6.85(s, 2H, **B** Ar−CH); 3.45(s, 4H, NH_2); 2.25-(m, 20H, **B** Me, **B** c-hexyl); 2.10(s, 12H, **B** Me); 1.65−1.55(m, 12H, **B** c-hexyl). δ_C in $CDCl_3$ (ppm): 165.3; 148.7; 140.1; 137.7; 134.8; 134.7; 131.0; 130.3; 129.1; 127.2; 127.1; 126.9; 126.0; 121.6; 44.9; 37.2; 26.5; 23.0; 18.7; 18.1. FAB[+ve] m/z = 775, $C_{52}H_{62}N_4O_2$ requires 774. IR in KBr disk (cm^{-1}): 3431; 2933; 2858; 1654; 1492.

H$_2$N−BIBIB−NH$_2$: mp 243 °C. δ_H in d_6-DMSO (ppm): 9.80(s, 4H, NH); 8.50(s, 2H, **I** Ar−CH); 8.15(d, 4H, **I** Ar−CH); 7.65(t, 2H, **I** Ar−CH); 7.10(s, 2H, **B** Ar−CH); 7.00(s, 2H, **B** Ar−CH); 6.80(s, 2H, **B** Ar−CH); 4.35(s, 4H, NH_2); 2.25(m, 8H, **B** c-hexyl); 2.20(s, 12H, **B** Me); 2.16(s, 12H, **B** Me); 2.07(s, 12H, **B** Me); 1.65−1.55(m, 12H, **B** c-hexyl). δ_C in $CDCl_3$ (ppm): 165.6; 165.5; 148.6; 147.3; 140.0; 137.8; 135.6; 135.0; 133.7; 131.8; 131.1; 127.1; 121.7; 44.8; 18.7; 18.0. FAB-[+ve] m/z = 1228, $C_{82}H_{94}N_6O_4$ requires 1226. IR in KBr disk (cm^{-1}): 3425; 2934; 2858; 1654; 1493.

Synthesis of TBIB−NH$_2$. Et_3N (2.89 mmol; 0.4 mL) and **H$_2$N−B−NH$_2$** (2.89 mmol; 2.23 g) were dissolved in dry CH_2Cl_2 (50 mL), and to this solution was added dropwise over 2 h *tert*-butyl benzoyl chloride (0.41 mmol; 77 μl) in dry CH_2Cl_2 (100 mL). The reaction was then allowed to stir for 8 h. The reaction mixture was then made up to 500 mL by adding CH_2Cl_2 and extracted with 1 M HCl (2 × 500 mL). The aqueous phase was made basic with NaOH pellets and extracted with CH_2Cl_2 (3 × 300 mL). The organic solvent was then removed on a rotary evaporator. Flash column chromatography on silica, eluting with 50% ethyl acetate/pet ether (40−60), yielded the desired product as the first band. The product was recrystallized from CH_2Cl_2/pet ether (196 mg; 51%) to give a white solid; mp 210−211 °C. δ_H in $CDCl_3$ (ppm): 8.45(s, 1H, **I** Ar−CH); 7.95(m, 2H, **I** Ar−CH); 7.80(m, 3H, NH, **T** Ar−CH); 7.70(s, 1H, NH); 7.45(m, 3H, NH, **T** Ar−CH); 7.23(t, 1H, **I** Ar−CH); 7.05(s, 2H, **B** Ar−CH); 7.03(s, 2H, **B** Ar−CH); 7.00(s, 2H, **B** Ar−CH); 6.85(s, 2H, **B** Ar−CH); 3.45(bs, 2H, NH_2); 2.20(m, 14H, **B** Me, **B** c-hexyl); 2.17(s, 6H, **B** Me); 2.10(s, 6H, **B** Me); 1.65−1.55(m, 12H, **B** c-hexyl); 1.35(s, 9H, **T** C$\underline{Me}_3$). δ_C in $CDCl_3$ (ppm): 166.1; 165.5; 165.4; 155.2; 148.6; 147.3; 140.1; 137.7; 135.3; 134.9; 134.3; 134.1; 131.6; 131.4; 131.3; 131.1; 130.5; 128.8; 127.2; 127.1; 126.9; 126.0; 125.5; 121.5; 45.0; 44.9; 37.3; 36.9; 34.9; 26.5; 23.0; 18.8; 18.7; 18.1. FAB[+ve] m/z = 936, $C_{63}H_{74}N_4O_3$ requires 934. IR in KBr disk (cm^{-1}): 3431; 2935; 2859; 1654; 1493; 1376.

Synthesis of TBIBT. Et_3N (6.38×10^{-4} mol; 0.1 mL) and **H$_2$N−BIB−NH$_2$** (3.19×10^{-4} mol; 247 mg) were dissolved in dry CH_2Cl_2 (75 mL). *tert*-Butyl benzoyl chloride (6.38×10^{-4} mol; 0.12 mL) was then added and the reaction allowed to stir for 4 h. The reaction was then washed with 1 M HCl (2 × 50 mL) and 1 M NaOH (2 × 50 mL) before being dried over Na_2SO_4 (anhydrous). The Na_2SO_4 was removed by filtration and the solvent removed under reduced pressure. Flash column chromatography on silica, eluting with 2% EtOH/CH_2Cl_2, gave the desired product as the second band. The first band was impurity. The product was recrystallized form CH_2Cl_2/pet ether (40−60) to give a white solid (302 mg; 86%); mp 239−240 °C. δ_H in d_6-DMSO (ppm): 9.80(s, 2H, NH); 9.55(s, 2H, NH); 8.53(s, 1H, **I** Ar−CH); 8.15-(d, 2H, **I** Ar−CH); 7.92(d, 4H, **T** Ar−CH); 7.68(t, 1H, **I** Ar−CH); 7.55(d, 4H, **T** Ar−CH); 7.15(s, 8H, **B** Ar−CH); 2.35−2.25(m, 8H, **B** c-hexyl); 2.2(s, 12H, **B** Me); 2.17(s, 12H, **B** Me) 1.60−1.55(m, 12H, **B** c-hexyl); 1.35(s, 18H, **T** C$\underline{Me}_3$). δ_C in $CDCl_3$ (ppm): 165.9; 155.0; 147.5; 147.1; 135.1; 131.6; 131.4; 127.2; 126.9; 125.4; 45.0; 36.8; 34.9; 31.2; 26.3; 22.9; 18.7;18.6. FAB[+ve] m/z = 1096, $C_{74}H_{85}N_4O_4$ requires 1094 IR in $C_2H_2Cl_4$ solution (cm^{-1}): 3422; 2982; 2970; 2939; 2863; 1670; 1609; 1491.

Synthesis of TBIBIA. TBIB−NH$_2$ (1.07×10^{-4} mol; 100 mg) and Et_3N (2.68×10^{-4} mol; 37 μl) were dissolved in dry CH_2Cl_2 (10 mL), and the **AI−COCl** (2.14×10^{-4} mol; 73 mg) in dry CH_2Cl_2 (10 mL) was added dropwise over 20 min. The reaction was then allowed to stir for 4 h. The solvent was then removed under reduced pressure on the rotary evaporator. The desired product was separated by preparative TLC eluting with 2% EtOH/CH_2Cl_2 to yield the product as the lowest band. Recrystallization from CH_2Cl_2/MeOH/Pet ether (40−60) gave a white solid (122 mg; 92%); mp 252−253 °C. δ_H in d_6-DMSO (ppm): 9.92(s, 1H, NH); 9.80(m, 3H, NH); 9.55(s, 1H, NH); 8.52(s, 1H, **I** Ar−CH); 8.50(s, 1H, **I** Ar−CH); 8.25−8.10(m, 4H, **I** Ar−CH); 7.90-(d, 2H, **T** Ar−CH); 7.75−7.62(m, 2H, **I** Ar−CH); 7.52(d, 2H, **T** Ar−CH); 7.32(t, 1H, **A** Ar−CH); 7.21(d, 2H, **A** Ar−CH); 7.15−7.07(m, 8H, **B** Ar−CH); 3.14(sept, 2H, **A** C$\underline{H}$Me$_2$); 2.35−2.25(m, 8H, **B** c-hexyl); 2.23−2.12(m, 24H, **B** Me); 1.60−1.45(m, 12H, **B** c-hexyl); 1.39(s, 9H, **T** C$\underline{Me}_3$); 1.22−1.10(2d, 12H, **A** CH$\underline{Me}_2$). δ_C in 5% CD_3-OD in $CDCl_3$ (v/v) (ppm): 165.8; 147.3; 146.6; 135.6; 134.5; 134.3;

131.7; 131.0; 127.2; 126.7; 125.3; 123.4; 44.7; 37.0; 31.4; 28.7; 23.5; 22.7; 18.7. FAB[+ve] m/z = 1243, $C_{83}H_{94}N_5O_5$ requires 1240. IR in $C_2H_2Cl_4$ solution (cm^{-1}): 3419; 3318; 2998; 2980; 2968; 2938; 2863; 1664; 1584; 1501; 1470.

Synthesis of AIBIBIA. AI−COCl (8.95×10^{-4} mol; 306 mg) was taken up in dry CH_2Cl_2 (25 mL), and to this solution were added **H_2N−BIB−NH_2** (4.48×10^{-4} mol; 346 mg) and Et_3N (8.95×10^{-4} mol; 0.13 mL) in dry CH_2Cl_2 (25 mL). The reaction was allowed to stir for 3 h. Flash column chromatography on silica, eluting with 1.5% EtOH/CH_2Cl_2, gave the product as the second band. Recrystallization from CH_2Cl_2/MeOH/pet ether (40−60) gave the product as a white solid (378 mg; 55%); mp 260−261 °C. δ_H in d_6-DMSO (ppm): 9.90(s, 2H, NH); 9.80(m, 4H, NH); 8.55(s, 2H, **I** Ar−CH); 8.50(s, 1H, **I** Ar−CH); 8.25−8.12(m, 6H, **I** Ar−CH); 7.70(t, 3H, **I** Ar−CH); 7.32(t, 2H, **A** Ar−CH); 7.22(d, 4H, **A** Ar−CH); 7.13(s, 8H, **B** Ar−CH); 3.12-(sept, 2H, **A** C$\underline{H}$Me$_2$); 2.35−2.25(m, 8H, **B** c-hexyl); 2.23−2.16(m, 24H, **B** Me); 1.60−1.45(m, 12H, **B** c-hexyl); 1.22−1.10(2d, 24H, **A** CH$\underline{Me}_2$). δ_C in d_6-DMSO (ppm): 166.2; 165.1; 147.1; 146.6; 135.5; 132.9; 130.5; 129.2; 127.5; 126.6; 123.5; 45.2; 28.7; 24.0; 23.2; 19.0. FAB[+ve] m/z = 1391, $C_{92}H_{104}N_6O_6$ requires 1388. IR in $C_2H_2Cl_4$ solution (cm^{-1}): 3419; 3317; 2993; 2971; 2937; 2865; 1665; 1602; 1584; 1500; 1470.

Synthesis of TBIBIBT. Et_3N (9.84×10^{-4} mol; 0.14 mL) and **H_2N−BIBIB−NH_2** (4.92×10^{-4} mol; 605 mg) were dissolved in dry CH_2Cl_2 (75 mL), and to this solution was added *tert*-butyl benzoyl chloride (9.84×10^{-4} mol; 0.2 mL). The reaction was allowed to stir for 10 hours. The reaction mixture was then washed with 1 M HCl (2 × 100 mL), 1 M NaOH (2 × 100 mL), and H_2O (2 × 100 mL) before being dried over Na_2SO_4 (anhydrous). Na_2SO_4 was then removed by filtration and the organic solution reduced to dryness on a rotary evaporator. The product was isolated by recrystallizing from CH_2Cl_2/MeOH/pet ether (40−60) giving a white solid (672 mg; 88%); mp 270−271 °C. δ_H in 5% CD_3OD in $CDCl_3$ (v/v) (ppm): 8.52(s, 2H, **I** Ar−CH); 7.97-(d, 4H, **I** Ar−CH); 7.84(d, 4H, **T** Ar−CH); 7.50(d, 4H, **T** Ar−CH); 7.20−7.05(m, 14H, **I** Ar−CH, **B** Ar−CH); 2.35−2.15(m, 48H, **B** Me, **B** c-hexyl); 1.65−1.50(m, 18H, **B** c-hexyl); 1.39(s, 18H, **T** C$\underline{Me}_3$). δ_C in d_6-DMSO (ppm): 165.3; 165.1; 154.7; 147.3; 147.1; 146.9; 135.6; 135.5; 135.3; 133.2; 132.9; 132.1; 130.6; 129.1; 127.8; 127.4; 126.6; 125.7; 45.2; 36.6; 31.4; 26.5; 23.2; 19.0. FAB[+ve] m/z = 1547, $C_{104}H_{118}N_6O_6$ requires 1546. IR in $C_2H_2Cl_4$ solution (cm^{-1}): 3421; 3307; 3002; 2980; 2970; 2938; 2862; 1664; 1603; 1492.

General Procedure for Solid-Phase Synthesis of Zippers. Three hundred milligrams of the Novasyn K HMPB resin (Novabiochem, 0.09 mMol/g) was dried overnight under vacuum in the presence of silica gel as a desiccant. The resin was then placed in a dry pipet and washed with 5 mL of dry dichloromethane. A solution of 1 mmol of the reagent in 7 mL of dry DCM and 360 μL of pyridine was prepared for each synthetic step. This solution was run through the resin five times. The excess of reagent was removed by washing with 7 mL of dry DCM, and the procedure was repeated for the next reagent. When the synthesis was complete, the resin was washed with 10 mL of methanol and dried under vacuum. The cleavage of the zippers was carried out by washing the resin with 20 mL of a solution of DCM/TFA (9:1) twice and then 10 mL of DCM and 10 mL of methanol. The fractions were combined and neutralized with solid sodium hydrogen carbonate, washed with water and dried over anhydrous Na_2SO_4. The solvent was removed on a rotary evaporator, and the white-yellow residue was analyzed by FAB mass spectrometry and ^{1}H NMR spectroscopy.

TBI−OH: δ_H in d_6-DMSO (ppm): 9.85 (s, 1H); 9.55 (s, 1H); 8.55 (s, 1H); 8.20 (d, 1H); 8.17 (d, 1H); 7.90 (d, 2H); 7.68 (t, 1H); 7.53 (d, 2H); 7.16 (s, 4H); 2.26 (m, 4H); 2.22 (s, 12H); 1.4 (m, 4 H); 1.27 (s, 9H). FAB[+ve] m/z = 631, $C_{41}H_{46}N_2O_4$ requires 630.

TBIBI−OH: δ_H in d_6-DMSO (ppm): 9.80 (s, 2H); 9.76 (s, 1H); 9.51 (s, 1H); 8.49 (s, 1H); 8.45 (s, 1H); 8.14 (m, 6H); 7.87 (t, 1H); 7.63 (m, 4H); 7.49 (d, 2H); 7.06 (s, 8H); 2.25 (m, 8H); 2.11 (m, 24H); 1.5 (m, 8H); 1.26 (s, 9H). FAB[+ve] m/z = 1084, $C_{71}H_{79}N_4O_6$ requires 1083.

^{1}H NMR Dilution Experiments. A sample of known concentration (of the order 10−100 mM) in a chosen solvent ($CDCl_3$ or $CDCl_3/CD_3OD$) was prepared, and a ^{1}H NMR spectrum was recorded on a 0.8 mL sample. From this sample, 0.4 mL was removed and replaced by 0.4 mL of solvent. After shaking to mix the solvents, a second ^{1}H NMR spectrum was recorded. This procedure was repeated until there was no further change in chemical shift or the sample was too dilute to record a spectrum (10^{-5} M). For signals that moved more than 0.01 ppm over the whole concentration range, the chemical shifts at each concentration were recorded and fitted to a dimerization or polymerization isotherm using purpose written software on an Apple Macintosh microcomputer, *NMRDil_Dimer* or *NMRDil_Agg*. These programs use a Simplex procedure to fit the experimental data to the following equations to determine the optimum solutions for the association constant, and the bound and free chemical shifts.

NMRDil_Dimer fits the data to a dimerization isotherm by solving the following equations.

$$[AA] = \frac{1 + 4K_d[A]_0 - \sqrt{\{1 + 8K_d[A]_0\}}}{8K_d} \quad (1)$$

$$[A] = [A]_0 - 2[AA] \quad (2)$$

$$\delta_{obs} = \frac{2[AA]}{[A]_0}\delta_d + \frac{[A]}{[A]_0}\delta_f \quad (3)$$

where

$[A]_0$ is the total concentration

[A] is the concentration of unbound free species

[AA] is the concentration of dimer

K_d is the dimerization constant

δ_f is the free chemical shift

δ_d is the limiting bound chemical shift of the dimer

NMRDil_Agg fits the data to a noncooperative linear polymerization isotherm by solving the following equations.

$$[Agg] = [A]_0\left\{1 - \frac{2}{1 + \sqrt{\{1 + 4K[A]_0\}}}\right\} \quad (4)$$

$$[A] = [A]_0 - [Agg] \quad (5)$$

$$\delta_{obs} = \frac{[Agg]}{[A]_0}\delta_b + \frac{[A]}{[A]_0}\delta_f \quad (6)$$

where

$[A]_0$ is the total concentration

[A] is the concentration of sites which are unbound (this is the sum of the free species and the ends of the aggregate which are not bound)

[Agg] is the concentration of sites involved in intermolecular interactions in the aggregate

K is the association constant for chain extension of the aggregate

δ_f is the free chemical shift

δ_b is the limiting bound chemical shift of the bound sites in the aggregate

Dilution experiments were also performed on mixtures of compounds, especially when the zipper complex was very stable. In this case, samples of the compounds, arbitrarily designated host and guest, were accurately weighed and mixed in an approximately 1:1 molar ratio. This mixture was then dissolved in an accurately measured volume

of solvent (typically to give a 25 mM solution). ^{1}H NMR spectra were recorded with progressive dilution of the sample as outlined above. The dilution data were fit to a 1:1 binding isotherm using purpose written software an Apple Macintosh microcomputer, *NMRDil_HG*. This program use a Simplex procedure to fit the experimental data to the following equation to determine the optimum solutions for the association constant, the bound chemical shift in the HG complex, and if required, the free chemical shift of the unbound species.

$$[HG] = \frac{1 + K[H]_0[G]_0 - \sqrt{\{(1 + K[H]_0[G]_0)^2 - 4K^2[H]_0[G]_0\}}}{2K} \quad (7)$$

$$[H] = [H]_0 - [HG] \quad (8)$$

$$\delta_{obs} = \frac{[HG]}{[H]_0}\delta_b + \frac{[H]}{[H]_0}\delta_f \quad (9)$$

where

$[H]_0$ is the total concentration of host

$[G]_0$ is the total concentration of guest

[H] is the concentration of unbound free host

[HG] is the concentration of host·guest complex

K is the association constant for formation of the host·guest complex

δ_f is the free chemical shift of the host

δ_b is the limiting bound chemical shift of the host·guest complex

^{1}H NMR Titration Experiments. A 3.0 mL sample of host of known concentration was prepared in a chosen solvent ($CDCl_3$ or $CDCl_3/CD_3OD$). The concentration of the host solution was chosen so that the host was not significantly dimerized (determined from the dilution experiment). A portion (0.8 mL) of this solution was removed, and a ^{1}H NMR spectrum was recorded. An accurately weighed sample of the guest was then dissolved in the remaining 2.2 mL of host solution. This solution was almost saturated with guest to allow access to the top of the binding isotherm and contained host so that the host concentration remained constant during the titration. Aliquots of guest solution were added successively to the NMR tube containing the host solution, the tube was shaken to mix the host and guest solutions, and the ^{1}H NMR spectra were recorded after each addition. For signals that moved more than 0.01 ppm, the chemical shifts at all concentrations of guest were recorded and analyzed using purpose-written software on an Apple Macintosh microcomputer, *NMRTit_HG*, *NMRTit_HGG*, or *NMRTit_HG+HH+GG*. These programs use a Simplex procedure to fit the data to the appropriate binding model to yield the association constant, the bound chemical shift in the HG complex, and if required, the free chemical shift of the unbound species.

NMRTit_HG and *NMRTit_HGG* was described in detail elsewhere.[11]

NMRTit_HG+HH+GG fits the data to a 1:1 binding isotherm for formation of the host·guest complex but in addition takes into account the presence of dimeriation equilibria for both the host and guest. The method starts by assuming that [HG] = 0, so that eqs 10 and 11 can be solved exactly for [HH] and [GG]. These values of are then used to solve eq 12 for [HG]. Equations 13 and 14 give the concentrations of free host [H] and free guest [G]. At this point, $[H] + [HH] + [HG] \neq [H]_0$, and $[G] + [GG] + [HG] \neq [G]_0$, so that the value of [HG] from eq 12 is used in eqs 10 and 11 to reevaluate [HH] and[GG], and the procedure is carried out repetitively until $[H] + [HH] + [HG] = [H]_0$, and $[G] + [GG] + [HG] = [G]_0$. This allows the set of simultaneous equations to be solved for the concentrations of all species present.

$$[HH] = \frac{1 + 4K_{dH}([H]_0 - [HG]) - \sqrt{\{1 + 8K_{dH}([H]_0 - [HG])\}}}{8K_{dH}} \quad (10)$$

$$[GG] = \frac{1 + 4K_{dG}([G]_0 - [HG]) - \sqrt{\{1 + 8K_{dG}([G]_0 - [HG])\}}}{8K_{dG}} \quad (11)$$

$$[HG] = \frac{1 + K([G]_0 - [GG])([H]_0 - [HH])}{2K} - \frac{\sqrt{\{(1 + K([G]_0 - [GG])([H]_0 - [HH]))^2 - 4K^2([G]_0 - [GG])([H]_0 - [HH])\}}}{2K} \quad (12)$$

$$[H] = [H]_0 - 2[HH] - [HG] \quad (13)$$

$$[G] = [G]_0 - 2[GG] - [HG] \quad (14)$$

$$\delta_{obs} = \frac{[HG]}{[H]_0}\delta_b + \frac{2[HH]}{[H]_0}\delta_d + \frac{[H]}{[H]_0}\delta_f \quad (15)$$

where

[HH] is the concentration of host dimer

[GG] is the concentration of guest dimer

K_{dG} is the guest dimerization constant

K_{dH} is the host dimerization constant

δ_d is the limiting bound chemical shift of the host dimer

All experiments were performed at least twice. The association constant for a single run was calculated as the mean of the values obtained for each of the signals followed during the titration weighted by the observed changes in chemical shift. The association constants from different runs were then averaged. Errors are quoted at the 95% confidence limits (twice the standard error). For a single run, the standard error was determined using the standard deviation of the different association constants determined by following different signals. The curve-fitting programs described above are available from the author on request.

Job Plot Experiments. For each component of the complex, 10 mL solutions of accurately measured and identical concentrations (in the range 6−10 mM) were prepared. The two solutions were then combined to give a series of samples of identical total concentration but conatining different mole fractions (χ) of the two components. The ^{1}H NMR spectrum of each sample was then recorded, and these spectra were used to produce a graph of ($\Delta\delta \times \chi$) against χ, the Job plot ($\Delta\delta = \delta_{observed} - \delta_{\chi=1.0}$).[15]

Acknowledgment. We thank the EPSRC (A.P.B.), the University of Sheffield (F.J.C.), the New Zealand government (A.E.R.), the Spanish government (C.R.), and the Lister Institute (C.A.H.) for financial support.

Supporting Information Available: X-ray crystal structure data for **AIA** (PDF). This material is available free of charge via the Internet at http://pubs.acs.org.

JA0012671

(15) Job, P. *Ann. Chim.* **1928**, *113*, 113−116.